Asymmetric Buckling of Toroidal Shells Under Axial Tension

S. K. RADHAMOHAN* AND B. PRASAD*
Vikram Sarabhai Space Center, Trivandrum, India

A theoretical study of asymmetric buckling of toroidal shells under axial tension is covered in this paper. Sanders nonlinear theory is used in formulating the buckling and prebuckling equations. The nonlinear differential equations encountered in the prebuckling analysis are solved, by "parametric differentiation technique" recently used for solving axisymmetric buckling problems. The axial tensile deformation at the truncated boundary of the shell is chosen as the parameter in the above technique. The buckling behavior for various ratios of radius to thickness of the toroid is investigated. The buckling load gradually increases with increasing thickness of the toroid but the circumferential waves decrease rapidly. The effect of boundary conditions on the buckling behavior of a truncated hemisphere is also studied and compared with the existing results.

Nomenclature

a = radius of the parallel circle at the clamped edge of the toroidal shell
E = Young's modulus of elasticity
E_o = reference modulus of elasticity
F = axial tensile load per unit circumferential length at the shell equator
G = modulus of rigidity
L = reference length of the shell
M_s, M_θ = moments in meridional and circumferential directions, respectively
n = number of circumferential waves
N_s, N_θ = normal stress resultants along meridional and circumferential directions, respectively
$\hat{N}_{s\theta}$ = effective shear at boundary
$N_{s\theta}, M_{s\theta}$ = inplane shear force and twisting moment
Q_s, Q_θ = radial shear forces
$\hat{Q}_s$ = effective radial shear
q_s, q_θ, q = surface forces acting along meridional, circumferential and radial directions, respectively
r = radius of parallel circle
R = reference radius of the shell
R_s, R_θ = principal radii of curvature in s and θ directions, respectively
s = the distance measured along the shell surface
t = thickness of the shell
t_o = reference thickness
u, v, w = the displacements in meridional, circumferential and normal directions, respectively
$\bar{Z}_u$ = nondimensionalized height of the truncated shell
θ = circumferential angle measured from a reference surface
ν = Poisson's ratio
α_o = altitude angle of the truncated edge
δ = axial deformation at the truncated edge
$\phi_s, \phi_\theta, \phi$ = rotations of the reference surface
$\varepsilon_s, \varepsilon_\theta$ = normal strains in s and θ directions, respectively
ψ_s, ψ_θ = curvatures of the reference surface
$\varepsilon_{s\theta}$ = shearing strain
$\psi_{s\theta}$ = twisting curvature
$\bar{(\ )}$ = nondimensionalized quantities
$(\ )_o$ = prebuckling quantities
$(\ )^*$ = perturbed quantities

Introduction

TOROIDAL, hemispherical, and torispherical shells are widely used as end domes in aerospace structures such as boosters and re-entry vehicles. From headroom considerations, toroidal and torispherical domes are preferred to hemispherical ones. Stability analysis of these shells of revolution based on consistent approach[1] was carried out using different numerical methods such as Finite Difference,[2,3] Integration[4] and Finite Element Methods.[5,6] Since these theoretical values did not agree with the experimental results, attention was given to the study of geometrical imperfections on the buckling behavior.[7,8]

It has been established theoretically and experimentally[14] that a torispherical shell buckles under internal pressure with large number of circumferential waves. Another situation in which buckling is predominant is a toroid under axial tension. This problem, although an interesting one, has not been dealt with so far. Some attempts have, however, been made recently on the study of buckling behavior of truncated hemispherical shells under axial tension, using different numerical techniques. Yao[9] analyzed the above problem using Vlasov's small deflection theory. The equations of equilibrium and compatibility conditions were satisfied by the use of Galerkin's approximation. The same problem was investigated by Navaratna and others[5] using a finite element technique (comprising of 30 equal size elements) with clamped boundary conditions. Theoretical predictions of this method were reported to be very close to the experimental values of Yao.[9] In his numerical solution Wu[10] used consistent buckling approach of Stein[1] in conjunction with Finite Difference iteration scheme for solving both the prebuckling and eigenvalue problem. The buckling strengths were found to be in good agreement with Yao's[9] membrane results.

Though the results of membrane and bending prebuckling analyses agree very well in the case of hemispherical shells, such a conclusion cannot be taken for granted for toroidal shells whose actual behavior is represented by a bending state. Hence in the present work, the prebuckling state is idealized by a nonlinear bending state. Sanders[15] nonlinear shell theory is adopted to derive both the (nonlinear) prebuckling and (linear) buckling equations.

Parametric differentiation technique has been used here for solving the nonlinear differential equations of the prebuckling state. This method was used recently in the investigation of axisymmetric buckling of spherical shells.[11,12] In the above cases, external load on the shell was chosen as a parameter for solving the nonlinear differential equations. However, in this investigation, the axial deformation at the truncated edge of the toroidal shell is used to demonstrate the generality of parametric differentiation technique. The method is explained below.

The nonlinear differential equations are first differentiated with respect to this parameter and the order of differentiation between the space variable and the deformation parameter is then interchanged. This leads to a system of linear differential equations with variable coefficients, the new dependent variables being the gradients with respect to the deformation parameter. The problem thus reduces to the solution of a linear boundary value problem along space (independent) variable and an initial value problem along the deformation parameter.

The linear boundary value problem can be solved by con-

Received May 10, 1973; revision received September 24, 1973.
Index category: Structural Stability Analysis.
* Engineer, Structural Engineering Division.

verting it to a set of initial value problems through "segmentation technique."[13] Higher order Runge-Kutta method with Gill's variation is employed here to integrate the initial value problems. The theoretical study treats the case where both the truncated edge and the clamped edge are restrained from moving radially or from rotating.

Governing Equations

The strain displacement and equilibrium equations are chosen from Sanders' nonlinear formulation, applicable to thin shells of revolution.[15] The rotations are assumed to be moderately small so that squares of rotation are retained in the strain displacement relations. Stress strain laws based on Kirchhoff-Love hypothesis are chosen. The material is assumed to be homogeneous and isotropic. The positive directions of displacements, stress resultants and external forces are shown in Fig. 1.

Since it is more convenient to deal with nondimensionalized quantities in numerical computation, the following nondimensionalization is adopted

$$\begin{aligned}
(\bar{u}, \bar{v}, \bar{w}, \bar{t}) &= (u, v, w, t)/t_o \\
(\bar{r}, \bar{R}_\theta) &= (r, R_\theta)/R \\
(\bar{s}, \bar{R}_s) &= (s, R_s)/L \\
(\bar{\psi}_\theta, \bar{\psi}_{s\theta}) &= (\psi_\theta, \psi_{s\theta})R \\
\bar{\psi}_s &= \psi_s L \\
(\bar{N}_s, \bar{N}_\theta, \bar{N}_{s\theta}, \bar{Q}_s, \bar{Q}_\theta) &= (N_s, N_\theta, \hat{N}_{s\theta}, \hat{Q}_s, Q_\theta)/E_o t_o \\
(\bar{M}_s, \bar{M}_\theta, \bar{M}_{s\theta}) &= (M_s, M_\theta, M_{s\theta})/E_o t_o^2 \\
(\bar{q}_s, \bar{q}_\theta, \bar{q}) &= (q_s, q_\theta, q)/E_o
\end{aligned} \tag{1}$$

The governing equations are rearranged into a set of eight first-order equations so that they can be readily integrated by "Runge-Kutta" Method. This arrangement of equations easily takes care of the variations in the loading and material properties. The variables which specify the boundary conditions at any $\bar{s}$ = const edge, are chosen as the dependent variables and hence the boundary conditions can be satisfied without any difficulty.

Buckling Criteria

The "adjacent configuration" approach, is used to derive the buckling equations from the above nonlinear differential equations. The adjacent configuration differing infinitesimally from the primary state (prebuckling state) can be written as

$$\begin{aligned}
\bar{u}_f &= u_o(\bar{s}) + u^*(\bar{s}, \theta) \\
\bar{v}_f &= v^*(\bar{s}, \theta) \\
\bar{w}_f &= w_o(\bar{s}) + w^*(\bar{s}, \theta)
\end{aligned} \tag{2}$$

where u_o, w_o are the displacements prior to incipient of buckling, and u^*, v^*, w^* are the additional quantities which are assumed to be infinitesimal.

The terms involving linear functions of these additional displacements are retained in the equations. The corresponding strains, curvatures and stress resultants of the adjacent state can be written in a similar way.

Assuming that the prebuckling state is an axisymmetric state, the corresponding equations governing this state can be identified from the adjacent equilibrium state. The final equations (written in first order form) in terms of the prebuckled and perturbed quantities are given below.

Prebuckling Equations

$$\begin{aligned}
du_o/d\bar{s} &= (L/t_o)[(\varepsilon_{so} - (t_o/L)(w_o/\bar{R}_s) - \phi_{so}^2/2)] \\
dw_o/d\bar{s} &= u_o/\bar{R}_s - (L/t_o)\phi_{so} \\
d\phi_{so}/d\bar{s} &= \psi_{so} \\
dN_{so}/d\bar{s} &= (\bar{r}'/\bar{r})(N_{\theta o} - N_{so}) - Q_{so}/\bar{R}_s - (L/t_o)\bar{q}_s \\
dQ_{so}/d\bar{s} &= N_{so}/\bar{R}_s + (L/R)N_{\theta o}/\bar{R}_\theta - (L/t_o)\bar{q}(\bar{s}) - (\bar{r}'/\bar{r})Q_{so} \\
dM_{so}/d\bar{s} &= (\bar{r}'/\bar{r})(M_{\theta o} - M_{so}) + (L/t_o)Q_{so} + (L/t_o)\phi_{so}N_{so}
\end{aligned} \tag{3}$$

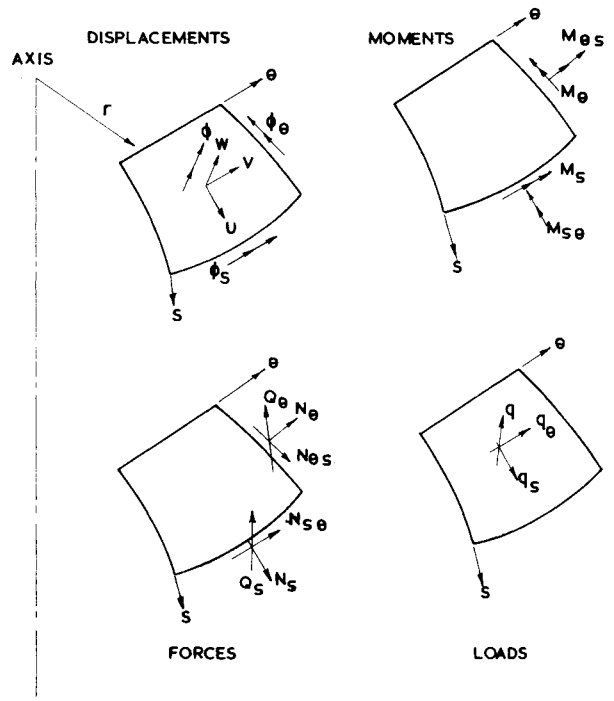

Fig. 1 Sign convention for displacements, stress resultants, and forces.

where

$$\begin{aligned}
\varepsilon_{\theta o} &= (t_o/L)\bar{r}'u_o/\bar{r} + (t_o/R)(w_o/\bar{R}_\theta) \\
\psi_{\theta o} &= (R/L)\bar{r}'\phi_{so}/\bar{r} \\
\varepsilon_{so} &= N_{so}[(1-\nu^2)/\bar{E}\bar{t}] - \nu\varepsilon_{\theta o} \\
N_{\theta o} &= \bar{E}\bar{t}/(1-\nu^2)(\varepsilon_{\theta o} + \nu\varepsilon_{so}) \\
\psi_{so} &= (L/t_o)\{[12(1-\nu^2)/\bar{E}\bar{t}^3]M_{so} - \nu(t_o/R)\psi_{\theta o}\} \\
M_{\theta o} &= [\bar{E}\bar{t}^3/12(1-\nu^2)][(t_o/R)\psi_\theta - \nu(t_o/L)\psi_{so}]
\end{aligned} \tag{4}$$

The boundary conditions at $\bar{s}$ = const are

$$\begin{aligned}
N_{so} \quad &\text{or} \quad u_o \\
Q_{so} \quad &\text{or} \quad w_o \\
M_{so} \quad &\text{or} \quad \phi_{so}
\end{aligned} \tag{5}$$

Buckling Equations

The perturbed quantities are functions of $\bar{s}$ and θ. Since our area of interest is only shells of revolution, these quantities can be expressed in terms of periodic functions in θ direction. Thus

$$\begin{aligned}
u^*(\bar{s}, \theta) &= \sum_{n=1}^{\infty} u_n^* \operatorname{cosn}\theta \\
v^*(\bar{s}, \theta) &= \sum_{n=1}^{\infty} v_n^* \operatorname{sinn}\theta \\
w^*(\bar{s}, \theta) &= \sum_{n=1}^{\infty} w_n^* \operatorname{cosn}\theta
\end{aligned} \tag{6}$$

All other quantities are expanded in a similar manner. In Eqs. (6), n corresponds to number of waves in the circumferential direction. The final equations in terms of perturbed quantities are

$$\begin{aligned}
dN_{sn}^*/d\bar{s} &= (\bar{r}'/\bar{r})(N_{\theta n}^* - N_{sn}^*) + (2/\bar{r})(L/R)(t_o/R)(n/\bar{R}_\theta)M_{s\theta n}^* - \\
&\quad Q_{sn}^*/\bar{R}_s + (L/R)(n/\bar{r})(N_{so} + N_{\theta o})\phi_n^* - \\
&\quad (L/R)(n/\bar{r})N_{s\theta n}^* - (L/t_o)q_s^* \\
dN_{s\theta n}^*/d\bar{s} &= (L/R)v_{\theta n}^*/\bar{R}_\theta + (t_o/R)M_{s\theta n}^*(1/\bar{R}_\theta)' + [N_{s\theta n}^* - \\
&\quad \{(t_o/R)(3/\bar{R}_\theta) - (t_o/L)(1/\bar{R}_s)\}]M_{s\theta n}^*/2 - \\
&\quad [\phi_n^*(N_{so} + N_{\theta o})/2][(L/R)\phi_{so}/\bar{R}_\theta - 2\bar{r}'/\bar{r}] + \\
&\quad (L/R)(n/\bar{r})N_{\theta n}^* + (L/R)N_{\theta o}\phi_{\theta n}^*/\bar{R}_\theta - (L/t_o)q_\theta^*
\end{aligned} \tag{7}$$

$$
\begin{aligned}
dQ_{sn}^*/d\bar{s} &= N_{sn}^*/\bar{R}_s+(L/R)N_{\theta n}^*/\bar{R}_\theta+(L/R)(n/\bar{r})[N_{\theta o}\phi_{\theta n}^*+\\
&\quad \phi_{so}\langle N_{s\theta n}^*-\{(t_o/R)(3/\bar{R}_\theta)-(t_o/L)(1/\bar{R}_s)\}M_{s\theta n}^*/2-\\
&\quad \phi_n^*(N_{so}+N_{\theta o})/2\rangle]-(\bar{r}'/\bar{r})Q_{sn}^*+(n/\bar{r})(L/R)\times\\
&\quad v_{\theta n}^*-(L/t_o)q^*\\
dM_{sn}^*/d\bar{s} &= (\bar{r}'/\bar{r})(M_{\theta n}^*-M_{sn}^*)+(L/t_o)Q_{sn}^*-\\
&\quad (L/R)(2n/\bar{r})M_{s\theta n}^*+(L/t_o)(\phi_{so}N_{sn}^*+\phi_{sn}^*N_{so})\\
du_n^*/d\bar{s} &= (L/t_o)[\varepsilon_{sn}^*-(t_o/L)w_n^*/\bar{R}_s-\phi_{so}\phi_{sn}^*]\\
dv_n^*/d\bar{s} &= (L/t_o)[2\varepsilon_{s\theta n}^*+(t_o/R)(n/\bar{r})u_n^*+(t_o/L)\bar{r}'v_n^*/\bar{r}-\\
&\quad \phi_{so}\phi_{\theta n}^*]\\
d\phi_{sn}^*/d\bar{s} &= \psi_{sn}^*\\
dw_n^*/d\bar{s} &= -(L/t_o)\phi_{sn}^*+u_n^*/\bar{R}_s
\end{aligned}
$$

where

$$
\begin{aligned}
\varepsilon_{\theta n}^* &= (t_o/L)\bar{r}'u_n^*/\bar{r}+(t_o/R)w_n^*/\bar{R}_\theta+(t_o/R)(n/\bar{r})v_n^*\\
\psi_{\theta n}^* &= (n/\bar{r})\phi_{\theta n}^*+(R/L)\bar{r}'\phi_{sn}^*/\bar{r}\\
\psi_{s\theta n}^* &= \tfrac{1}{2}[R/L(d\phi_{\theta n}^*/d\bar{s})-(n/\bar{r})\phi_{sn}^*-(R/L)\bar{r}'\phi_{\theta n}^*/\bar{r}+\\
&\quad (1/\bar{R}_\theta-(R/L)/\bar{R}_s)\phi_n^*]\\
\phi_{\theta n}^* &= (t_o/R)(nw_n^*/\bar{r}+v_n^*/\bar{R}_\theta)\\
\phi_n^* &= \tfrac{1}{2}[(t_o/L)(dv_n^*/d\bar{s})+(t_o/L)\bar{r}'v_n^*/\bar{r}+(t_o/R)(n/\bar{r})u_n^*]\\
\varepsilon_{sn}^* &= [(1-\nu^2)/\bar{E}\bar{t}]N_{sn}^*-\nu\varepsilon_{\theta n}^*\\
N_{\theta n}^* &= [\bar{E}\bar{t}/(1-\nu^2)](\varepsilon_{\theta n}^*+\nu\varepsilon_{sn}^*)\\
\psi_{sn}^* &= (L/t_o)[\{12(1-\nu^2)/\bar{E}\bar{t}^3\}M_{sn}^*-\nu(t_o/R)\psi_{\theta n}^*]\\
M_{\theta n}^* &= [\bar{E}\bar{t}^3/12(1-\nu^2)][(t_o/R)\psi_{\theta n}^*+\nu(t_o/L)\psi_{sn}^*]\\
N_{s\theta n}^* &= \{(t_o/R)(3/\bar{R}_\theta)-(t_o/L)(1/\bar{R}_s)\}M_{s\theta n}^*/2+(N_{so}+N_{\theta o})\times\\
&\quad \phi_n^*/2+\bar{G}\bar{t}\psi_{s\theta n}^*\\
M_{s\theta n}^* &= (\bar{G}\bar{t}^3/12)(t_o/R)\psi_{s\theta n}^*
\end{aligned}
\tag{8}
$$

In the above equations, q_s^*, q_θ^*, q^* are the perturbed quantities of the external load. In the case of dead loading all these quantities are zero because the load vector remains invariant. In the case of normal pressure field ($\bar{q}$) whose magnitude remains unaltered but the direction changes depending on the normal, these quantities are

$$
\begin{aligned}
q_s^* &= \bar{q}\phi_{sn}^*\\
q_\theta^* &= \bar{q}\phi_{\theta n}^*\\
q^* &= \bar{q}(e_{sn}^*+e_{\theta n}^*)
\end{aligned}
\tag{9}
$$

where

$$
\begin{aligned}
e_{sn}^* &= \varepsilon_{sn}^*-\phi_{so}\phi_{sn}^*\\
e_{\theta n} &= \varepsilon_{\theta n}^*
\end{aligned}
$$

The boundary conditions at $\bar{s}$ = const are

$$
\begin{aligned}
N_{sn}^* = 0 \quad \text{or} \quad u_n^* = 0\\
N_{s\theta n}^* = 0 \quad \text{or} \quad v_n^* = 0\\
Q_{sn}^* = 0 \quad \text{or} \quad w_n^* = 0\\
M_{sn}^* = 0 \quad \text{or} \quad \phi_{sn}^* = 0
\end{aligned}
\tag{10}
$$

The nonlinear Eqs. (3) along with Eqs. (4) and (5), governing the prebuckling state are solved by "Parametric Differentiation Technique." The dependent variables of this integration enter into Eqs. (7–9) as variable coefficients. The integration of linear homogeneous Eqs. (7) and (8) with homogeneous boundary conditions [Eqs. (10)] can be carried out by assuming unit values in succession for the unspecified quantities at one end. Finally at the far end, a set of homogeneous boundary conditions is to be satisfied. Hence for a nontrivial solution, the determinant formed by the corresponding coefficients of the homogeneous integrations should vanish. When the determinant changes sign between two successive values of the deformation parameter, a linear interpolation along with a finer step size of the parameter near the bifurcation point can be used to find the more accurate bifurcation load. The wave number which corresponds to the minimum value of the axial deformation, near the bifurcation point is taken as a harmonic wave number at buckling.

A computer program using the above formulation and methods of solution has been developed to obtain the asymmetric buckling loads of thin shells of revolution.[16] The program has the capability to tackle different types of loading and boundary conditions. An input variable in the main routine distinguishes between the linear and nonlinear bending states in the prebuckling analysis. If linear bending state is assumed, the "Parametric Differentiation" scheme is skipped and the equations are directly integrated by "Segmentation Technique" coupled with "Runge-Kutta" method. Minor modifications are made in the above program to get the numerical results in the present investigation.

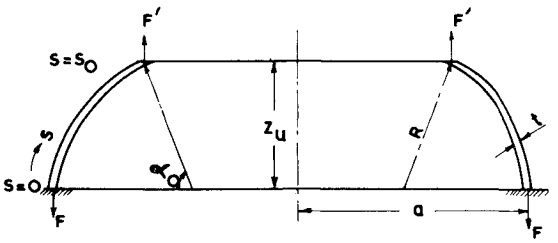

Fig. 2 Shell geometry.

Numerical Results and Discussion

In order to verify the formulation, the buckling loads for a truncated hemispherical (special case of toroid) shell under tension are obtained. The geometry is the same as adopted by Wu.[10] The boundary conditions are chosen as

Prebuckling state

$$
\begin{aligned}
u_o = w_o = \phi_{so} = 0 \quad \text{at} \quad \bar{s} = 0\\
u_o = (\delta/t)\cos\alpha_o; \quad w_o = (\delta/t)\sin\alpha_o; \quad \phi_{so} = 0 \text{ at } \bar{s} = 1
\end{aligned}
$$

Buckling state

$$
u_n^* = v_n^* = w_n^* = \phi_{sn}^* = 0 \quad \text{at} \quad \bar{s} = 0 \quad \text{and} \quad \bar{s} = 1 \tag{11}
$$

The results of the present investigation agree very well with Wu's[10] work. The buckling strengths and the corresponding wave numbers of this investigation are listed in Table 1 along with the results of other investigators. The same problem is analyzed by Yao[9] and Navaratna[5] by using a different set of boundary conditions for the buckled state. They are

$$
w_n^* = \phi_{sn}^* = N_{sn}^* = N_{s\theta n}^* = 0 \quad \text{at} \quad \bar{s} = 0 \quad \text{and} \quad \bar{s} = 1 \tag{12}
$$

The values for this case do not differ from the analysis based on Eq. (11). The results of the present theory with the changed boundary conditions agree with Yao,[9] but deviate considerably from the work of Ref. 5. This observation requires a fresh investigation of the above problem with a more refined finite element formulation.

Toroidal Shell Under Tension

The toroidal shell geometry (Fig. 2) is chosen with α_o equal to 23° 30′ and $a = 1440$, where "a" is the radius of the parallel circle at the clamped edge. The shell thickness is altered and the buckling stresses are obtained for different R/t ratios. The boundary conditions as given by Eq. (11) are used here.

Table 1 Buckling load for a truncated hemisphere under axial tension[a]

Harmonic number	Dimensionless buckling load $[F/Et] \times 10^4$				
	Galerkin method[9]	Finite element method[5]	Finite difference method[10]	Parametric differentiation technique	Experimental[9]
38	...	7.00	...	12.97	...
39	...	6.88	...	12.93	6.15
40	13.4903	6.93	13.0567	13.16	...

[a] $a/t = 480$ and $Z_u = 0.39875$.

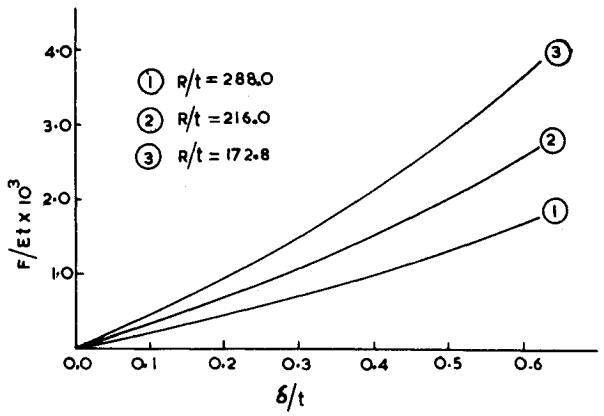

Fig. 3 F/Et vs δ/t for different values of R/t.

The prebuckling results indicate that the variation of F/Et (where F is the meridional stress at the clamped edge) is nonlinear with respect to δ/t. This variation is shown in Fig. 3 for three representative ratios of R/t. It can be observed that this nonlinear behavior becomes predominant for smaller values of R/t. The variation of normal deformation prior to buckling is shown in Fig. 4. Most of the shell deforms inwardly except a small portion near $\bar{s} = 1$ edge which has outward deformation.

Table 2 Buckling of a toroidal shell under axial tension[a]

Geometric parameter	Harmonic wave no.	Critical axial tensile load	Critical axial extension
R/t	n	$F/Et \times 10^3$	δ/t
288.0	43	1.403	0.5201
247.0	40	1.75	0.5223
216.0	39	2.15	0.52661
192.1	36	2.755	0.55461
172.8	35	3.495	0.5875
157.2	34	5.175	0.6921
154.4	33	5.55	0.71189

[a] Shell geometry: $a = 1440$; $Z_a = 0.39875$; $\alpha_0 = 23° 30'$; $R = 864$.

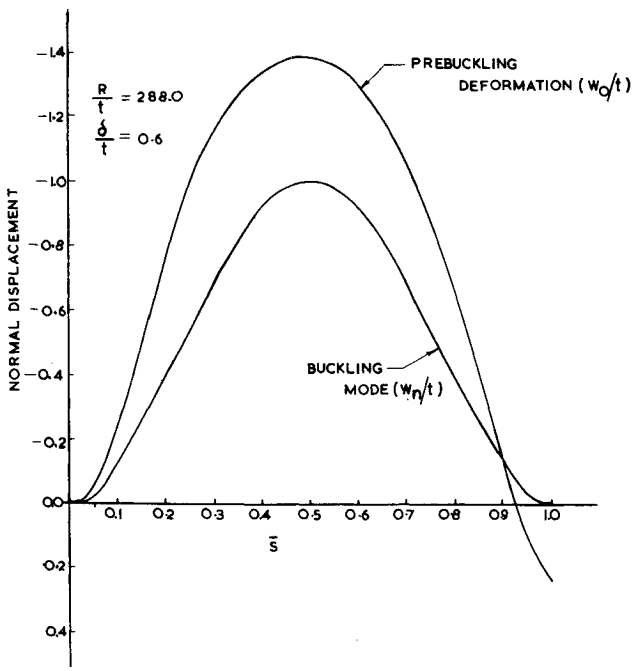

Fig. 4 Buckling mode and the corresponding prebuckling deformation for a typical shell geometry.

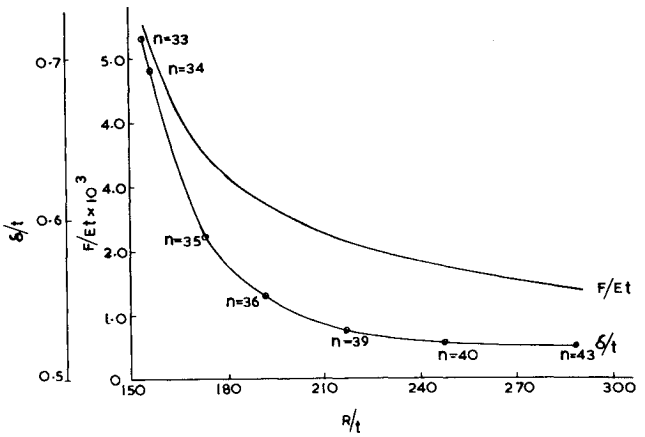

Fig. 5 Critical axial deformation and stress at the clamped edge for various shell geometries.

The buckling stresses for various ratios of R/t are given in Table 2 and plotted in Fig. 5. The results show that the dimensionless critical load decreases as R/t increases. However, the decrease is very rapid in the range $150 < R/t < 190$ and gradual for $R/t > 190$. The circumferential waves increase as R/t increases. The variation of the critical value of δ/t with respect to R/t is also shown in Fig. 5. The circumferential stresses at the inner and outer faces of the toroid prior to buckling are plotted in Fig. 6. It can be observed that the inner face of the shell is completely under compression while the outer face is subjected to tensile stress at the boundaries.

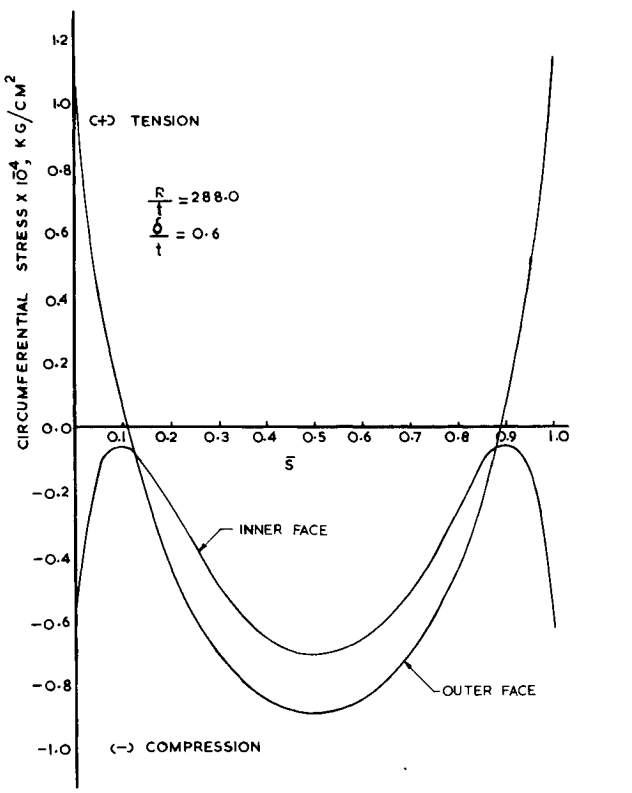

Fig. 6 Variation of circumferential stress along the toroidal surfaces prior to buckling.

This shows that except for the edge zones, the whole section in the remaining part of the shell is under compression which causes instability. However, the meridional stresses are found to be tensile in the interior region of the shell; except at the boundaries. A representative mode shape for $R/t = 288$ is plotted in Fig. 4.

Conclusions

Choosing the axial deflection at the truncated edge of a shell as a parameter, the parametric differentiation technique is used for the first time to obtain the asymmetric buckling loads of a toroid under axial tension. The different boundary conditions considered here do not affect the buckling phenomena of hemispherical shells even when the prebuckling state is represented by a general nonlinear bending state. For a toroid under tension, the variation between meridional stress and δ/t is nonlinear and is more predominant for lower values of R/t. The buckling phenomena is caused because of the compressive circumferential stresses, existing over a large part of the shell. Buckling stresses decrease more rapidly when R/t values are small. However, the wave numbers increase with increasing R/t.

References

[1] Stein, M., "Some Recent Advances in the Investigation of Shell Buckling," *AIAA Journal*, Vol. 6, No. 12, Dec. 1968, pp. 2339–2345.

[2] Bushnell, D., "Symmetric and Nonsymmetric Buckling of Finitely Deformed Eccentrically Stiffened Shells of Revolution," *AIAA Journal*, Vol. 5, No. 8, Aug. 1967, pp. 1455–62.

[3] Almroth, B. O. and Bushnell, D., "Computer Analysis of Various Shells of Revolution," *AIAA Journal*, Vol. 6, No. 10, Oct. 1968, pp. 1848–55.

[4] Radhamohan, S. K., "Nonlinear Stability of Thin Shells of Revolution," Ph.D. thesis, June 1971, Department of Civil Engineering, Indian Institute of Technology, Kanpur, India.

[5] Navaratna, D. R., Pian, T. H. H., and Witmer, E. A., "Stability Analysis of Shells of Revolution by the Finite-Element Method," *AIAA Journal*, Vol. 6, No. 2, Feb. 1968, pp. 355–361.

[6] Stricklin, J. A., Haisler, W. E., MacDougall, H. R., and Stebbins, F. J., "Nonlinear Analysis of Shells of Revolution by Matrix Displacement Method," *AIAA Journal*, Vol. 6, No. 12, Dec. 1968, pp. 2306–12.

[7] Koiter, W. T., "Elastic Stability and Post-Buckling Behavior," *Proceedings of Symposium on Nonlinear Problems*, edited by Langer, Univ. of Wisconsin Press, Madison, Wisc., 1963, pp. 257–275.

[8] Hutchinson, J. W., "Imperfection Sensitivity of Externally Pressurized Spherical Shells," *Journal of Applied Mechanics*, Vol. 34, 1967, pp. 49–55.

[9] Yao, J. C., "Buckling of Truncated Hemisphere under Axial Tension," *AIAA Journal*, Vol. 1, No. 10, Oct. 1963, pp. 2316–2319.

[10] Wu, M. T. and Cheng, S., "Nonlinear Asymmetric Buckling of Truncated Spherical Shells," *Journal of Applied Mechanics, Transactions of ASME*, Vol. 37, Sept. 1970, pp. 651–660.

[11] Setlur, A. V. and Radhamohan, S. K., "Buckling of Shallow Spherical Shells by Parametric Differentiation Technique," *The Proceedings of the 13th Congress on Theoretical and Applied Mechanics*, Durgapur, India, Dec. 1968.

[12] Radhamohan, S. K., Setlur, A. V., and Goldberg, J. E., "Stability of Shells by Parametric Differentiation," *Journal of Structural Division, Proceedings of the ASCE*, Vol. 97, ST6, June 1971, pp. 1775–1790.

[13] Goldberg, J. E., "Computer Analysis of Shells," *Proceedings of Symposium on Theory of Thin Shells to Honor L. H. Donnell*, edited by D. Muster, Univ. of Houston, Houston, Tex., 1967, pp. 5–22.

[14] Mescall, J., "Stability of Thin Torispherical Shells under Uniform Internal Pressure," Collected papers on Instability of Shell Structures, NASA-TND 1510, 1962, pp. 671–692.

[15] Sanders, J. L., Jr., "Nonlinear Theories for Thin Shells," *Quarterly of Applied Mathematics*, Vol. 21, No. 1, 1963, pp. 21–36.

[16] Radhamohan, S. K. and Setlur, A. V., "Computer Program for Buckling Analysis of Thin Shells of Revolution," CE Report I-71, June 1971, Dept. of Civil Engineering, Indian Institute of Technology, Kanpur, India.